ACS Catalysis

Research Article

Cite This: ACS Catal. 2019, 9, 9953−9963

pubs.acs.org/acscatalysis

Pt/ZrO_2 Prepared by Atomic Trapping: An Efficient Catalyst for the Conversion of Glycerol to Lactic Acid with Concomitant Transfer Hydrogenation of Cyclohexene

Zhenchen Tang,[†] Pei Liu,[‡] Huatang Cao,[§] Sara Bals,[‡] Hero J. Heeres,[†] and Paolo P. Pescarmona*[,†]

[†]Chemical Engineering Group, Engineering and Technology Institute Groningen, University of Groningen, Nijenborgh 4, 9747 AG Groningen, The Netherlands

[‡]Electron Microscopy for Materials Science, University of Antwerp, Gronenenborgerlaan 171, 2020 Antwerp, Belgium

[§]Advanced Production Engineering Group, Engineering and Technology Institute Groningen, University of Groningen, Nijenborgh 4, 9747 AG Groningen, The Netherlands

Supporting Information

ABSTRACT: A series of heterogeneous catalysts consisting of highly dispersed Pt nanoparticles supported on nanosized ZrO_2 (20 to 60 nm) was synthesized and investigated for the one-pot transfer hydrogenation between glycerol and cyclohexene to produce lactic acid and cyclohexane, without any additional H_2. Different preparation methods were screened, by varying the calcination and reduction procedures with the purpose of optimizing the dispersion of Pt species (i.e., as single-atom sites or extra-fine Pt nanoparticles) on the ZrO_2 support. The Pt/ZrO_2 catalysts were characterized by means of transmission electron microscopy techniques (HAADF-STEM, TEM), elemental analysis (ICP-OES, EDX mapping), N_2-physisorption, H_2 temperature-programmed-reduction (H_2-TPR), X-ray photoelectron spectroscopy (XPS), and X-ray diffraction (XRD). Based on this combination of techniques it was possible to correlate the temperature of the calcination and reduction treatments with the nature of the Pt species. The best catalyst consisted of subnanometer Pt clusters (<1 nm) and atomically dispersed Pt (as Pt^{2+} and Pt^{4+}) on the ZrO_2 support, which were converted into extra-fine Pt nanoparticles (average size = 1.4 nm) upon reduction. These nanoparticles acted as catalytic species for the transfer hydrogenation of glycerol with cyclohexene, which gave an unsurpassed 95% yield of lactic acid salt at 96% glycerol conversion (aqueous glycerol solution, NaOH as promoter, 160 °C, 4.5 h, at 20 bar N_2). This is the highest yield and selectivity of lactic acid (salt) reported in the literature so far. Reusability experiments showed a partial and gradual loss of activity of the Pt/ZrO_2 catalyst, which was attributed to the experimentally observed aggregation of Pt nanoparticles.

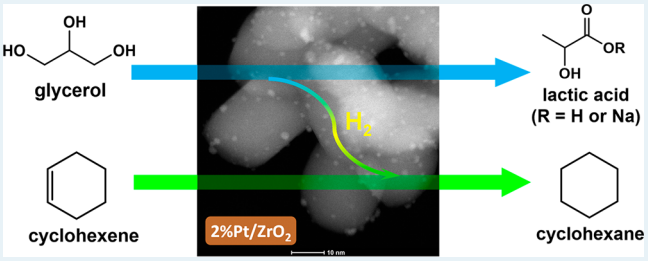

KEYWORDS: *glycerol, lactic acid, Pt catalyst, transfer hydrogenation, cyclohexene*

INTRODUCTION

Biomass is a renewable and, therefore, sustainable alternative to fossil resources such as oil, gas, and coal for the production of bulk and fine chemicals.[1−3] Glycerol is one of the most attractive biobased platform molecules due to the broad scope of chemical products that can be derived from it (e.g., lactic acid, acrolein, acrylic acid, and 1,2- and 1,3-propanediol) and due to its availability, which is a consequence of being the main side product of the manufacturing of biodiesel through transesterification of triglycerides from vegetable oils with methanol.[4,5] Therefore, the production of valuable fine and bulk chemicals from glycerol has attracted a lot of interest from both academia and industry.[6−8] Among the products that can be obtained from glycerol, lactic acid (LA) and alkyl lactates are attractive biobased platform molecules with several applications, ranging from the synthesis of the biodegradable poly lactic acid to the use as green solvents.[9] Lactic acid and lactates can be produced from glycerol through a dehydrogenation−rearrangement pathway (Scheme 1), which would provide a viable alternative to the current production of lactic acid by fermentation of carbohydrates.[4,9−12] The dehydrogenation−rearrangement of glycerol implies the nominal formation of H_2 (Scheme 1) and in this sense can be correlated to the use of glycerol as feedstock for the sustainable production of H_2 through an aqueous phase reforming (APR).[8,13,14] Hydrogen is widely used in the chemical industry (e.g., ammonia synthesis, Fischer−Tropsch process, steel industry, and various hydrogenation reactions) and in the fuel cell systems as a clean power source.[2,8,15] Clearly, routes that allow producing H_2 from a renewable source such as biomass represent a sustainable alternative to the current production

Received: May 23, 2019
Revised: August 30, 2019
Published: September 16, 2019

DOI: 10.1021/acscatal.9b02139
ACS Catal. 2019, 9, 9953−9963

Scheme 1. Catalytic Route from Glycerol to Lactic Acid Using Cyclohexene as Hydrogen Acceptor

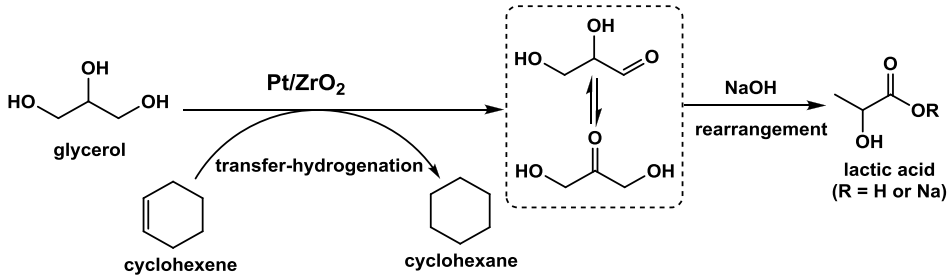

from fossil fuels through methane steam reforming, which requires extremely harsh conditions.[2,16]

The first reports on the conversion of aqueous glycerol into a lactic acid salt employed strongly basic solutions (NaOH and KOH in stoichiometric excess relative to glycerol) at high temperature (300 °C).[17−19] The combination of an excess of base and high temperature promoted the rate of dehydrogenation in the first step of the reaction network and the rate of the rearrangement in the second step by neutralizing the formed lactic acid. However, these conditions are not desirable for practical application or from the point of view of green chemistry. The reaction temperature can be lowered to 180 °C under He atmosphere by using a noble metal catalyst (Pt/C or Ir/C) in combination with a homogeneous base, reaching 95% conversion of glycerol and 55% selectivity toward lactic acid.[20,21] The oxidative dehydrogenation of glycerol can also be carried out in the presence of O_2, in which case water is the side-product. In this context, supported Au and its alloy catalysts ($AuPt/TiO_2$) in combination with NaOH gave 30% glycerol conversion and 86% selectivity to lactic acid at 90 °C.[17] More recent reports proved that the presence of a base is not essential under this oxidative atmosphere, with a bifunctional catalyst consisting of Pt supported on a zeolite (Sn-MFI) achieving an excellent 81% selectivity toward lactic acid at 90% conversion of glycerol under O_2 (6 bar) at a relatively mild temperature (90 °C).[10] Between the employed approaches, the path in the absence of O_2 allows generating valuable H_2 but requires relatively high temperature and a base to promote the dehydrogenation, whereas the reactions conducted under O_2 do not require a base (though at the cost of the turnover frequency per metal site) but the hydrogen atoms removed from glycerol react with oxygen to form a low-value product as water.[10]

A third approach that provides an attractive alternative to those described above consists in combining the dehydrogenation of glycerol with the hydrogenation of another compound. Few reports described the hydrogenation of cyclohexene or nitrobenzene using glycerol as hydrogen source, but focusing only on the efficiency of the hydrogenation step and not on that of the conversion of glycerol.[22−25] Here, we report a catalytic system that combines the dehydrogenation of glycerol and hydrogenation of cyclohexene over a Pt/ZrO_2 heterogeneous catalyst in a one-pot batch reaction under N_2 atmosphere (Scheme 1). We show that the careful design of the catalyst enables the efficient conversion of glycerol to lactic acid with much higher selectivity and under significantly milder conditions compared to those previously reported for the dehydrogenation of glycerol in the absence of O_2. Additionally, by performing the reaction in the presence of a model hydrogen acceptor as cyclohexene, we combined a very high lactic acid yield with the production of cyclohexane. In our catalyst design we selected Pt as active species, since this metal is highly active and, thus, widely used in hydrogenation and dehydrogenation reactions.[26] Since Pt is a very expensive element, it is of crucial importance to maximize the activity per gram of metal (and thus the turnover number). For this purpose, several preparation methods have been developed to obtain highly and uniformly dispersed Pt nanoparticles, such as wet-impregnation, sol-immobilization, and deposition-precipitation.[27−30] Very recently, a method based on atomic trapping was developed for the preparation of highly dispersed Pt, even at atomic level.[31−33] It was reported that the oxidized Pt species can disperse as single atoms on a CeO_{2-x} support upon calcination at 800 °C under air. The obtained catalyst showed excellent catalytic performance in the low-temperature oxidation of CO and in the conversion of methane into C_2 hydrocarbons.[34,35] Only a few kinds of supports (i.e., CeO_{2-x}, TiO_2, and nitrogen doped carbon) were found to promote such dispersion of Pt species at atomic level.[31,35,36] Here, these concepts have been extended to the preparation of highly dispersed Pt species (as Pt^{2+} and Pt^{4+}) on a nanosized ZrO_2 (particle size between 20 and 60 nm; average size: 32 nm). This oxide was chosen because of the similarity of its coordination geometry (zirconium is coordinated to 7 oxygens) to that found in CeO_{2-x} (with $0 < x < 0.5$ as a consequence of the presence of Ce(III) along Ce(IV) species),[37] while its potential as support for atomically dispersed Pt species has not been explored yet.[38] The Pt species were converted into extra-fine Pt nanoparticles upon reduction by H_2, and this system was studied for the first time for the combined dehydrogenation of glycerol and hydrogenation of cyclohexene, achieving unsurpassed yield and selectivity of lactic acid.

EXPERIMENTAL SECTION

Materials. Glycerol (99%), 1,3-dihydroxyacetone dimer (97%), glyceraldehyde (90%), glycolic acid (99%), lactic acid (98%), pyruvic aldehyde (40 wt % in H_2O), cyclohexene (99%), cyclohexane (99.5%), sodium hydroxide (98%), benzene (99.9%), hexachloroplatinic acid ($H_2PtCl_6{\cdot}xH_2O$, 99.9%), zirconium oxide (nanopowder, <100 nm), cerium oxide (nanopowder), and titanium oxide (P25) were purchased from Sigma-Aldrich. Glyceric acid (20 wt % in H_2O) was purchased from TCI Chemicals. The H_2O used in this work was always of Milli-Q grade. All chemicals were used without further purification.

Catalyst Synthesis. A wet-impregnation method was used for the preparation of the Pt/ZrO_2 catalysts. Typically, ZrO_2 (2.0 g) was mixed with an aqueous solution of H_2PtCl_6 (4.5 g Pt per L), with the volume of the latter being tuned to the target loading of Pt, and the slurry was stirred at room temperature until the water was evaporated. The solid mixture

DOI: 10.1021/acscatal.9b02139
ACS Catal. 2019, 9, 9953−9963

was then dried at 100 °C in air overnight in an oven. The resulting solid was milled into a fine powder and then calcined in air (400, 550, or 800 °C, heating rate: 3 °C/min). The calcined catalysts were reduced in a tubular oven under H_2 flow (99.9%; 200 mL/min) at a selected temperature (100, 250, or 400 °C, heating rate 3 °C/min) for 2 h. Before removing the sample from the oven, the gas flow was switched to N_2 for 1 h to remove adsorbed H_2 from the catalyst surface. A typical catalyst prepared by this method was named as aPt/ZrO_2-b-Rc, in which a, b and c stand for the wt % loading of Pt (a), the calcination temperature (b), and the reduction temperature (c). In addition, the catalyst prepared with 2 wt % of Pt was also reduced directly at 250 °C under a H_2 flow for 2 h after overnight drying (without calcination). This catalyst was named 2Pt/ZrO_2-DR250.

Characterization of the Catalysts. Transmission electron microscopy (TEM) images were obtained using a CM12 (Philips) electron microscope operating at 120 keV. The samples were prepared by ultrasonication in ethanol, after which a droplet of the suspension was added to a carbon coated 400 mesh copper grid. The images were taken with a slow scanning CCD camera.

High-angle annular dark-field scanning transmission electron microscopy (HAADF-STEM) images and energy-dispersive X-ray spectroscopy (EDX) mapping were collected using an aberration-corrected cubed FEI Titan microscope operating at an acceleration voltage of 300 kV. The samples were prepared by suspending the material in ethanol and depositing drops of the suspension on a copper grid covered with a holey carbon film.

Nitrogen physisorption isotherms were measured at −196 °C using a Micromeritics ASAP 2420 apparatus. The Brunauer−Emmet−Teller (BET) method was used to calculate the specific surface area. The Barrett−Joyner−Halenda (BJH) method was used to calculate the pore volume.

Elemental analysis by inductively coupled plasma optical emission spectrometry (ICP-OES) was performed using a PerkinElmer Optima 7000 DV instrument to determine the actual Pt loadings in the catalysts.

X-ray photoelectron spectroscopy (XPS) analysis was carried out by mounting the catalysts on a conductive tape adhered to the XPS sample holder. No further treatment was carried out prior to the XPS measurement. The sample was loaded into the device, and the pressure was reduced below 1 × 10^{-7} mbar. The XPS measurements were performed using a Surface Science SSX-100 ESCA instrument equipped with a monochromatic Al Kα X-ray source ($h\nu$ = 1486.6 eV). During the measurement, the pressure was kept below 2 × 10^{-9} mbar in the analysis chamber. For acquiring the data, a spot diameter of 600 μm was used. The neutralizer was turned on, to avoid charging effects. All XPS spectra were analyzed using the Winspec software package developed by LISE laboratory, University of Namur, Belgium, including Shirley background subtraction and peak deconvolution.

Hydrogen-temperature-programmed reduction (H_2-TPR) measurements were performed on an Autochem II 2920 from Micromeritics. In a typical experiment, 80 mg of sample was pretreated at 500 °C (heating rate 10 °C/min) for 1 h in a flow of He (30 mL/min). Subsequently, the sample was cooled to 50 °C under the same flow of He. The reduction analysis was performed from 50 to 900 °C (10 °C/min) in a 30 mL/min flow of 5 vol % H_2 in He.

X-ray diffraction (XRD) measurements were performed on a D8 Advance Bruker diffractometer with Cu Kα_1 radiation (λ = 1.5418 Å). The XRD patterns were collected under 40 kV and 40 mA in the range 10°−80°.

Catalytic Tests. The catalytic tests were carried out in a 100 mL Parr stainless steel autoclave reactor equipped with a Teflon liner and an overhead stirrer. In a typical test, a predetermined amount of the Pt/ZrO_2 catalyst was loaded into the reactor together with an aqueous solution of glycerol (0.5 M in 20 mL), NaOH (0.015 mol), and cyclohexene (0.02 mol, as organic phase). The reaction was performed under N_2 (20 bar) for 4.5 h at 160 °C (heating time 0.5 h not counted) at a stirring speed of 800 rpm. Then, the reactor was depressurized and the biphasic liquid was separated into an aqueous and an organic phase, which were filtered to remove the catalyst. The organic phase was analyzed by gas chromatography using a Thermo Trace GC equipped with a Restek Stabilwax-DA column (30 m × 0.32 mm × 1 μm) and a FID detector. The aqueous phase was first neutralized and diluted by aqueous H_2SO_4 (1 M) and then analyzed by high performance liquid chromatography [HPLC, Agilent Technologies 1200 series, Bio-Rad Aminex HPX-87H 300 × 7.8 mm column, T = 60 °C, with 0.5 mM aqueous H_2SO_4 as eluent (flow rate: 0.55 mL/min) using a combination of refractive index detector and UV detector]. Each component was calibrated using solutions of the individual compound at 4 different concentrations. Selected catalytic tests were performed on three different batches of 2Pt/ZrO_2-550-R250, showing good reproducibility of the results (deviation in the lactic acid yield value within ±4%). For these experiments, the average value of the yield is reported.

For the catalyst recycling test, a small amount of the reaction mixture was collected for analysis and the remaining mixture was filtered to recover the catalyst. The catalyst was washed first with H_2O (20 mL) and then with ethanol (20 mL), and this procedure was repeated 3 times, after which the solid was dried overnight at 100 °C. The obtained solid was used for the next run in the recycling test.

Definitions

The glycerol conversion (Conv./%) is defined by eq 1:

$$\text{Conv.} = \frac{C_{(g,0)} - C_{(g)}}{C_{(g,0)}} \times 100\% \quad (1)$$

in which $C_{(g)}$ is the molar concentration of glycerol after a certain reaction time and $C_{(g,0)}$ is the initial glycerol concentration.

The yield of lactic acid (Y_{LA}) is defined by eq 2:

$$Y_{LA} = \frac{C_{(LA)}}{C_{(g,0)}} \times 100\% \quad (2)$$

in which $C_{(LA)}$ is the molar concentration of lactic acid after a certain reaction time and $C_{(g,0)}$ is the initial molar concentration of glycerol.

The product selectivity for a compound p is defined by eq 3:

$$S_p = \frac{C_{(p)}}{C_{(g,0)} - C_{(g)}} \times 100\% \quad (3)$$

in which $C_{(p)}$ is the molar concentration of a product after a certain reaction time.

The selectivity toward the transfer hydrogenation is defined by eq 4:

DOI: 10.1021/acscatal.9b02139
ACS Catal. 2019, 9, 9953−9963

$$S_{\text{transfer-H}} = n\frac{y(\text{cyclohexane}) - 2y(\text{benzene})}{\sum_i xy(\text{p}_i)} \times 100\% \quad (4)$$

in which n is the molar ratio between cyclohexene and glycerol in the reaction mixture; y(cyclohexane) is the yield of cyclohexane; y(benzene) is the yield of benzene—which is obtained from the dehydrogenation of cyclohexene, which most likely occurs as a disproportionation with formation of two cyclohexane molecules per benzene molecule; $y(\text{p}_i)$ is the yield of each product that is obtained from the dehydrogenative oxidation of glycerol, e.g. lactic acid, glyceric acid, or glycolic acid, and x is the number of H_2 that can be removed from glycerol by dehydrogenation to each possible product (i.e., x = 1 for lactic acid; x = 2 for glyceric acid; x = 3 for glycolic acid).

The term "lactic acid" is used in this article to describe the product obtained from the reaction mixture, which actually is sodium lactate (mixed with a small portion of lactic acid from hydrolysis).

RESULTS AND DISCUSSION

Synthesis and Characterization of the Pt/ZrO_2 Catalysts. With the aim of developing an active and selective heterogeneous catalyst for the dehydrogenation of glycerol combined with the hydrogenation of cyclohexene at relatively mild temperature, we designed a system in which the Pt actives species would be highly dispersed on nanosized ZrO_2 as support, possibly even as single atoms.[31,32,35] A series of Pt/ZrO_2 catalysts with different loading of the noble metal was prepared by wet-impregnation and calcination, and then reduced by H_2 in a tubular oven. The actual loadings of Pt determined by ICP-OES measurement (Table 1) were very similar to the theoretical ones and ranged between 0.6% and 8.4%. The BET surface area decreased only slightly after loading the ZrO_2 support with 2 wt % Pt (~10%, from 32 to 29 m^2/g), which indicates that the presence of Pt did not affect significantly the textural properties of ZrO_2.

Table 1. Pt Loading on the Pt/ZrO_2 Catalysts and Surface Area before and after Supporting Pt on ZrO_2[a]

Entry	Material	Pt loading/ wt %	Surface area/ (m^2/g)	Pt particle size/nm
1	ZrO_2	0	32	n.a.
2	0.5Pt/ZrO_2-550-R250	0.6	n.d.	0.8
3	1Pt/ZrO_2-550-R250	1.1	n.d.	1.2
4	2Pt/ZrO_2-550-R250	2.1	29	1.4
5	5Pt/ZrO_2-550-R250	4.8	n.d.	2.0
6	9Pt/ZrO_2-550-R250	8.4	n.d.	2.6

[a]n.d. = not determined; n.a. = not applicable.

HAADF-STEM and TEM were used to characterize the presence and size of Pt particle on ZrO_2 (Figure 1 and 2). Remarkably, clusters at the subnanometer scale and single atomic Pt were observed on the ZrO_2 support after calcination at 550 °C in air (2Pt/ZrO_2-550, Figure 1A, Figure 2A, B, and Figure S1). This demonstrates that the Pt species were highly and even atomically dispersed on ZrO_2 after calcination in air.[31,34] Upon subsequent reduction of this catalyst in H_2 (250 °C, 1 h), very small, well-dispersed Pt nanoparticles with an average particle size of 1.4 nm formed on the ZrO_2 surface (2Pt/ZrO_2-550-R250, Figure 1C and Figure 2C). On this sample, the size of Pt ranges from subnanometer clusters (from 0.35 nm) to nanoparticles (up to 2.5 nm). The dispersion behavior of Pt on ZrO_2 is very similar to that reported for Pt/CeO_{2-x}, Pt/CN (nitrogen-doped carbon) and Rh/ZrO_2 systems characterized by atomically dispersed Pt or Rh species.[31,32,39,40] The presence of atomically dispersed cationic Pt species in the material obtained by calcination but prior to reduction (2Pt/ZrO_2-550) is further supported by XPS analysis (Figure 3A), which evidenced that all Pt in this material was in the oxidized state, mainly as Pt^{2+} (at 72.7 eV, 84% peak area) and to a lesser extent as Pt^{4+} (75.0 eV, 16% peak area). No Pt^0 species were observed, confirming the absence of metallic nanoparticles. The oxidized Pt species existing as highly dispersed single atoms and very small clusters are probably coordinated to ZrO_2 through Pt−O−Zr bonds.[31,33,35,39,41−43] After reduction at 250 °C, the majority of the oxidized Pt species were reduced to Pt^0 (at 71.2 eV, 62% peak area, Figure 3B), in agreement with the formation of the metallic Pt nanoparticles observed in 2Pt/ZrO_2-550-R250. However, Pt^{2+} (at 72.7 eV, 33% peak area) and Pt^{4+} (at 75.0 eV, 5% peak area) species were still present in this catalyst.[31,43]

To investigate in more detail the effect of the temperature of the reduction step, 2Pt/ZrO_2-550 was also reduced at 100 and 400 °C under H_2 flow (Figure 1B and D). By increasing the temperature of the reduction process from 100 to 400 °C, the average size of Pt nanoparticles increased from 1.4 nm (100 °C) to 1.8 nm (400 °C). This result can be explained considering that a higher reduction temperature leads to a reduction of a larger fraction of the oxidized Pt species to metallic Pt, while it also promotes the growth of larger Pt nanoparticles. In the Pt/ZrO_2 catalyst that was reduced

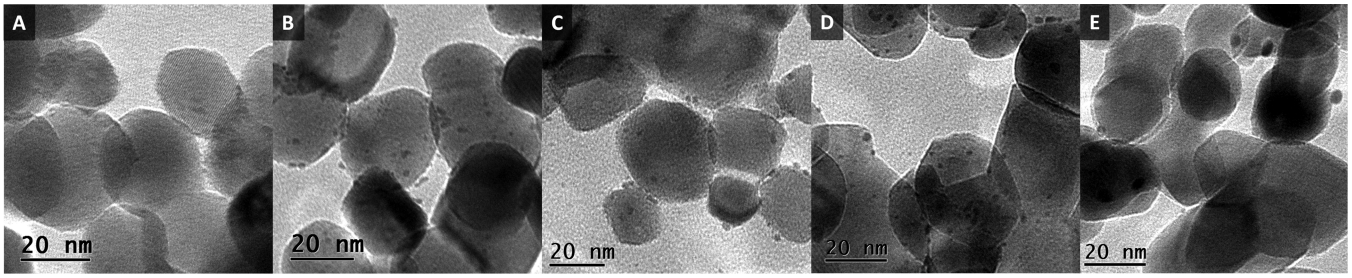

Figure 1. TEM images of 2Pt/ZrO_2 catalysts prepared by different calcination and reduction procedures. (A) 2Pt/ZrO_2-550; (B) 2Pt/ZrO_2-550-R100, average particle size of Pt: 1.4 nm; (C) 2Pt/ZrO_2-550-R250, average particle size of Pt: 1.4 nm; (D) 2Pt/ZrO_2-550-R400, average particle size of Pt: 1.8 nm; (E) 2Pt/ZrO_2-DR250, average particle size of Pt: 3.7 nm. Note: the resolution of these TEM images does not allow identification of nanoparticles <0.5 nm.

DOI: 10.1021/acscatal.9b02139
ACS Catal. 2019, 9, 9953−9963

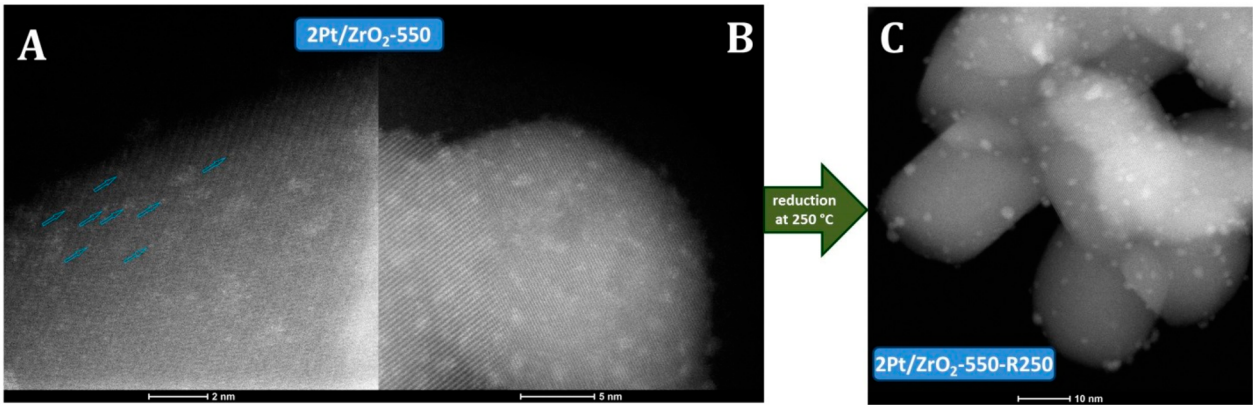

Figure 2. HAADF-STEM images of (A, B) the $2Pt/ZrO_2$ catalyst calcined at 550 °C ($2Pt/ZrO_2$-550) and (C) the same material after reduction at 250 °C ($2Pt/ZrO_2$-550-R250). In image (A), the arrows point to the single atom Pt species.

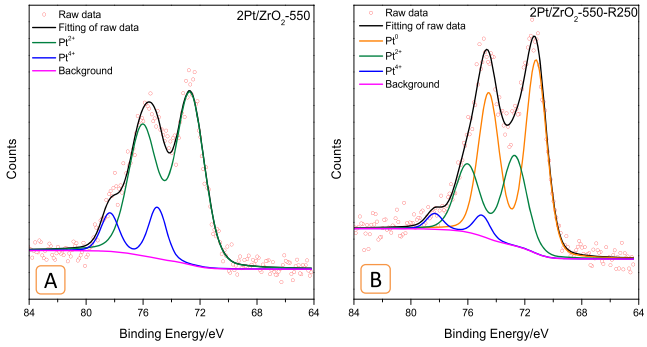

Figure 3. Pt 4*f* XPS signals of various Pt/ZrO_2 catalysts. (A) $2Pt/ZrO_2$-550, area of Pt^{2+} peak, 84%; area of Pt^{4+} peak, 16%; (B) $2Pt/ZrO_2$-550-R250, area of Pt^0 peak, 62%; area of Pt^{2+} peak, 33%; area of Pt^{4+} peak, 5%.

directly at 250 °C by H_2 without a previous calcination step, only a few Pt particles were observed on the surface of ZrO_2 (Figure 1E), and these display a significantly larger average size (3.7 nm) compared to those in $2Pt/ZrO_2$-550-R250 (1.4 nm). This suggests that the calcination process strongly enhances the chemical interaction between oxidized Pt species and ZrO_2, which is critical for the subsequent formation of extra-fine Pt nanoparticles upon reduction.

Considering the crucial role exerted by the calcination step on the state and size of the Pt species on the catalyst, we decided to study the effect of different calcination temperatures (400 and 800 °C, compared to 550 °C discussed above) on the dispersion of Pt species on ZrO_2. The catalysts were reduced at 250 or 400 °C in a H_2 flow after the calcination. The TEM images of $2Pt/ZrO_2$ calcined at 400 °C did not show any particles before reduction, while Pt nanoparticles with an average size of 2.0 nm were observed after reduction ($2Pt/ZrO_2$-400-R250, Figure S2A), which is slightly larger than the size of the nanoparticles in $2Pt/ZrO_2$-550-R250 (Figure 1C and 2B). On the other hand, when the calcination was carried out at 800 °C, only very large Pt particles (around 50 nm, determined by EDX-mapping) were observed before reduction ($2Pt/ZrO_2$-800, Figure 4A). Though not detected, a small fraction of Pt as single atoms might also be present, as suggested by the fact that after reduction at 400 °C a small amount of very fine Pt nanoparticles (~1 nm) was observed alongside the large Pt nanoparticles ($2Pt/ZrO_2$-800-R400, Figure 4C). These results are in agreement with previous

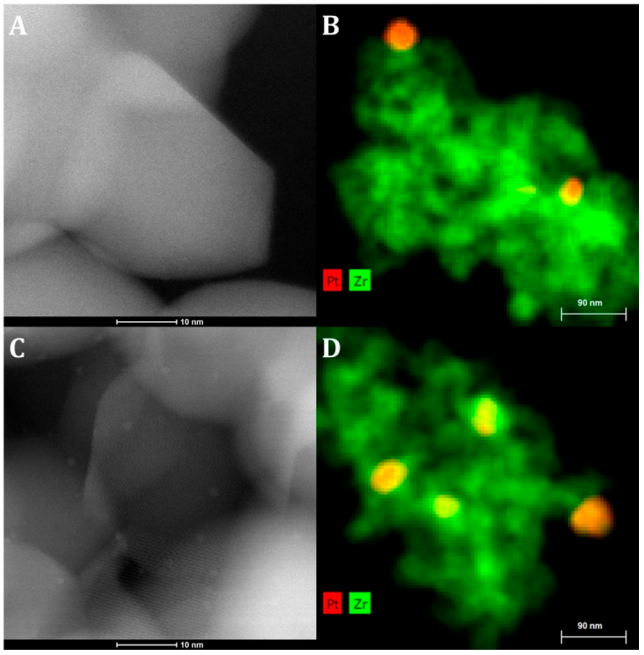

Figure 4. HAADF-STEM images (left) and EDX-mapping (right) of $2Pt/ZrO_2$ calcined at 800 °C (A and B, $2Pt/ZrO_2$-800) and the same material after reduction at 400 °C (C and D, $2Pt/ZrO_2$-800-R400). EDX-mapping: Zr: green; Pt: red.

reports, which showed that the calcination temperature can largely affect the interaction between Pt atoms and the oxide used as support.[33,36,40,44] The effect of decreasing the Pt loading to 0.5% on the nature of the Pt species was investigated by HAADF-STEM for the materials calcined at 550 or 800 °C (Figure S3). In $0.5Pt/ZrO_2$-550, subnanometer Pt clusters and even single atoms similar to those in $2Pt/ZrO_2$-550 were observed, though obviously in a lower amount. On the other hand, no Pt species could be detected in $0.5Pt/ZrO_2$-800 (Figure S3 and S4), which indicates that the lower Pt loading prevents the formation of the large Pt nanoparticles observed in the case of $2Pt/ZrO_2$-800 and that Pt most likely exists only as single atoms in this material.

The reducibility of $2Pt/ZrO_2$ as a function of the calcination temperature was investigated further by H_2-TPR from 50 to 800 °C (Figure 5). The intense peak in the 50−220 °C range and centered at 110 °C, which is visible in the TPR profiles of the materials calcined at 400 and 550 °C but is absent in that

DOI: 10.1021/acscatal.9b02139
ACS Catal. 2019, 9, 9953−9963

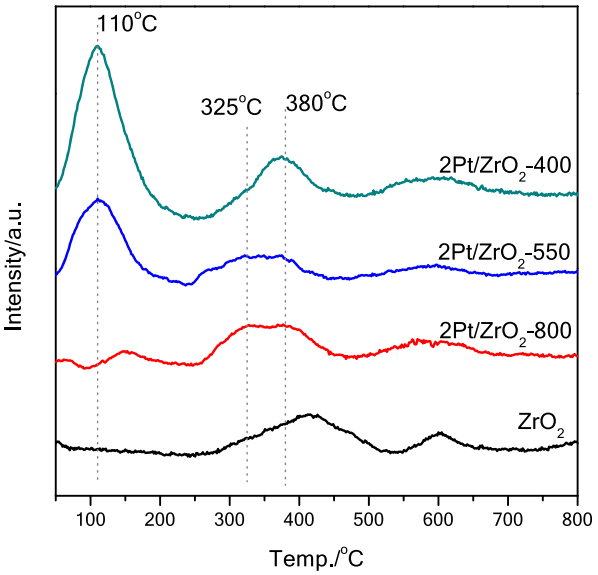

Figure 5. TPR profile of $2Pt/ZrO_2$ catalysts calcined at different temperatures (400, 550, and 800 °C) and of the support ZrO_2.

of the parent ZrO_2, is attributed to the reduction of oxidized Pt species.[40,41,45−48] The area of this peak becomes smaller when the calcination temperature increases. In the material calcined at 800 °C, the intensity of this peak is further decreased and its position is shifted to higher temperature (150 °C). This much lower tendency of $2Pt/ZrO_2$-800 to be reduced below 250 °C is in agreement with what was observed by TEM and HAADF-STEM (see Figure S2B and 4). This supports the hypothesis that the calcination at 800 °C promotes more efficiently the formation of highly dispersed and fully anchored oxidized Pt species in ZrO_2.[36,39] All H_2-TPR profiles present a broad signal ranging from 250 to 450 °C, which stems from two overlapping peaks centered at 325 and 380 °C (Figure 5). The peak at 325 °C can be ascribed to the reduction of remaining, oxidized Pt species (Pt^{2+} and Pt^{4+}), which based on the XPS data (*vide supra*) account for 38% of the Pt atoms in $2Pt/ZrO_2$-550-R250, i.e. after reduction at 250 °C.[41,48,49] The peak at 380 °C is ascribed to the reduction peaks of coordinatively unsaturated Zr^{4+} species at the surface of ZrO_2.[41] This peak is slightly shifted to lower temperature compared to the corresponding peak of the parent ZrO_2 (at 410 °C), which suggests that the presence of Pt species promotes the reduction of ZrO_2, possibly by hydrogen spillover.[41,50−52] The peak at 600 °C, which appeared in the profiles of all the samples, is ascribed to the reduction of (nearly) coordinatively saturated Zr^{4+} at surface terraces or in the bulk of ZrO_2.[41,52,53]

Next, we monitored the effect of the Pt loading on the features of the final catalyst, while keeping the temperature of the calcination (550 °C) and that of the reduction (250 °C) constant. Before reduction, Pt is present in the form of highly dispersed species with subnanometer size for Pt loading between 0.5 and 2% (Figure 2A,B and Figure S5A, B). With higher loadings (5% and 9%), small Pt nanoparticles with average size of 1.3 and 1.5 nm, respectively, were detected by TEM (Figure S5C,D). This suggests that a Pt loading ≥5% exceeds the maximum capacity of the ZrO_2 surface to host highly dispersed Pt species. The Pt atoms that cannot interact strongly with ZrO_2 aggregate as small nanoparticles.[40,54] After reduction at 250 °C under H_2 flow, Pt nanoparticles were observed for all samples (0.5−9Pt/ZrO_2-550-R250, Figure S6), and the average particle size gradually increased from 0.8 to 2.6 nm. This series of materials with different loadings of Pt on ZrO_2 (0.5−9Pt/ZrO_2) was further characterized by XRD (Figure S7). All XRD patterns display the characteristic peaks of monoclinic ZrO_2. No diffraction peaks due to Pt were observed on the Pt/ZrO_2 catalysts (before or after reduction) when the Pt loading was ≤5 wt %, whereas the characteristic peaks of metallic Pt (face centered cubic crystal) are observed for 9Pt/ZrO_2. This is due to both the small size and low loading of the Pt nanoparticles, which implies that the diffraction peaks of Pt are too broad and have too low intensity to be detected.

In summary, by systematically studying the effect of the Pt loading, the calcination temperature, and the reduction temperature, we can conclude that the formation of atomically dispersed Pt species on ZrO_2 is promoted by lower Pt loadings and by higher calcination temperatures. These conditions also lead to the formation of smaller nanoparticles upon reduction with H_2, with a smaller size being also favored by lower reduction temperature.

Catalytic Performance of the Pt/ZrO_2 Catalysts. The prepared Pt/ZrO_2 catalysts were tested for the conversion of glycerol to lactic acid using cyclohexene as the hydrogen acceptor (Scheme 1 and Table 2). Initially, $2Pt/ZrO_2$-550 (without reduction) was tested as catalyst for this reaction and showed 57% conversion of glycerol with 55% yield of lactic acid. The selectivity of the transfer hydrogenation ($S_{(Transfer-H)}$ in Table 2) was 31%, which means 31% of the hydrogen generated from the oxidation of glycerol was employed to reduce cyclohexene to cyclohexane (Entry 1 in Table 2). When the catalyst was reduced at 100 °C in H_2 flow, the catalytic results were very similar to the "unreduced" one (Entry 2,

Table 2. Catalytic Conversion of Glycerol to Lactic Acid Using a Pt/ZrO_2 Prepared with Different Reduction Methods[a]

					Selectivity in the conversion of glycerol (%)				Yield in the conversion of cyclohexene (%)[b]	
Entry	Catalyst	$Conv._{GLY}$ (%)	Y_{LA} (%)	$S_{(transfer-H)}$ (%)	Lactic acid	Glyceric acid	Glycolic acid	Propanediol	Cyclohexane	Benzene
1	$2Pt/ZrO_2$-550	57	55	35	97	0.9	0.5	1.8	8.9	0.5
2	$2Pt/ZrO_2$-550-R100	56	54	27	97	1.2	0.6	1.0	7.7	0
3	$2Pt/ZrO_2$-550-R250	96	95	36	99	0.5	0.2	0.7	17	0
4	$2Pt/ZrO_2$-550-R400	88	85	41	97	0.9	0.5	1.4	18	0
5	$2Pt/ZrO_2$-DR250	71	69	15	97	1.0	0.0	1.6	5.1	0

[a]Reaction conditions: aqueous glycerol solution: 10 mmol (0.5 M, 20 mL); cyclohexene: 20 mmol; nominal Pt/glycerol ratio = 1/1950; NaOH: 15 mmol; temperature: 160 °C; reaction time: 4.5 h; N_2 pressure: 20 bar. [b]Under the employed reaction conditions ($mol_{glycerol}$:$mol_{cyclohexene}$ = 1:2) the maximum theoretical yield of cyclohexane is 50%.

DOI: 10.1021/acscatal.9b02139
ACS Catal. 2019, 9, 9953−9963

Table 3. Catalytic Conversion of Glycerol to Lactic Acid Using Pt/ZrO_2 Catalysts Calcined at Different Temperatures[a]

					Selectivity in the conversion of glycerol (%)				Yield in the conversion of cyclohexene (%)[b]	
Entry	Catalyst	$Conv._{GLY}$ (%)	Y_{LA} (%)	$S_{(transfer\text{-}H)}$ (%)	Lactic acid	Glyceric acid	Glycolic acid	Propanediol	Cyclohexane	Benzene
1	$2Pt/ZrO_2$ 400-R250	46	46	35	99	0.3	0.0	0.8	8.1	0
2	$2Pt/ZrO_2$ 550-R250	96	95	36	99	0.5	0.2	0.7	17	0
3	$2Pt/ZrO_2$ 800-R250	24	23	0.9	98	0.3	0.0	1.9	0.1	0
4	$2Pt/ZrO_2$ 800-R400	12	10	0	87	0.7	0.7	11	0	0

[a]Reaction conditions: aqueous glycerol solution: 10 mmol (0.5 M, 20 mL); cyclohexene: 20 mmol; nominal Pt/glycerol ratio = 1/1950; NaOH: 15 mmol; temperature: 160 °C; reaction time: 4.5 h; N_2 pressure: 20 bar. [b]Under the employed reaction conditions ($mol_{glycerol}$:$mol_{cyclohexene}$ = 1:2) the maximum theoretical yield of cyclohexane is 50%.

Table 2). The TEM analysis showed a clear difference between the two catalysts (Figure 1), with no Pt nanoparticle being visible on the unreduced sample and very small, well-dispersed Pt nanoparticles appearing upon reduction at 100 °C in H_2 flow. Combining this with the catalytic results, we infer that the $2Pt/ZrO_2$-550 catalyst is reduced during the reaction. The catalyst prepared by reduction at 250 °C, $2Pt/ZrO_2$-550-R250, showed significantly higher conversion of glycerol (96%) and yield of lactic acid (95%), which is the highest yield of lactic acid from glycerol in the state of art (Entry 3, Table 2).[9,10,17,55] The selectivity in the transfer hydrogenation also increased, reaching 36%. When the reduction temperature of the catalyst was increased to 400 °C, the activity slightly decreased, with 88% glycerol conversion and 86% lactic acid yield (Entry 4, Table 2). All reactions produced minor amounts (<2%) of glyceric acid, glycolic acid, and propanediol as side products. For what concerns the conversion of cyclohexene, very high selectivity toward the hydrogenation to cyclohexane was observed, with no or minor dehydrogenation to benzene (Table 2). Combining the catalytic performance with the characterization results, it can be concluded that the highly dispersed oxidized Pt species, Pt^{2+} and Pt^{4+} (as determined by XPS and TPR), which are most abundant on the unreduced catalyst $2Pt/ZrO_2$-550, are probably not the active sites for the dehydrogenation of glycerol. These oxidized species are easily reduced to metallic Pt nanoparticles (Pt^0), which are highly active in catalyzing the dehydrogenation of glycerol, in line with several literature reports proving the hydrogenation/dehydrogenation activity of these species with a variety of substrates.[32,33,35,49,50,56,57] On the other hand, when the catalyst was directly reduced at 250 °C after wet-impregnation without prior calcination ($2Pt/ZrO_2$ DR250, Entry 5, Table 2), it showed much lower catalytic performance compared to the $2Pt/ZrO_2$ 550-R250. Combining these catalytic results with the TEM characterization, the activity trend can be correlated to the much larger and fewer Pt nanoparticles present on the surface of $2Pt/ZrO_2$-DR250. This underlines the importance of the calcination step in the preparation of highly dispersed, very small, and thus highly active Pt nanoparticles supported on ZrO_2.

The suitability of ZrO_2 as a support for Pt active species was further demonstrated by comparing the activity of $2Pt/ZrO_2$-550-R250 to that of analogous Pt-based catalysts prepared using TiO_2 or CeO_2 as support. Particularly, CeO_2 has been reported to promote the formation of atomically dispersed Pt species.[32,33,35] Our results indicate that the catalyst prepared using TiO_2 has significantly lower activity than its counterpart on ZrO_2, whereas the Pt catalyst supported on CeO_2 has slightly lower activity than the one on ZrO_2 (Table S1). Therefore, we focused the rest of our study on Pt/ZrO_2 catalysts.

The calcination temperature of Pt/ZrO_2 was found to affect significantly the size and dispersion of Pt species on the support (*vide supra*). These differences have a clear effect on the catalytic performance (Table 3). The Pt/ZrO_2 prepared by calcination at 400 °C and reduction at 250 °C ($2Pt/ZrO_2$-400-R250) showed 46% conversion of glycerol and 46% yield of lactic acid (Entry 1, Table 3), while $2Pt/ZrO_2$-550-R250 showed significantly higher conversion of glycerol (96%) and yield of lactic acid (95%) (Entry 2, Table 3). The improved activity is ascribed to the smaller size of the Pt nanoparticles in the latter catalyst (compare Figure 1C and Figure S2A). Further increase in the calcination temperature to 800 °C ($2Pt/ZrO_2$-800-R250) caused a drastic drop in activity (24% glycerol conversion, Entry 3, Table 3). Keeping the calcination temperature at 800 °C but increasing the reduction temperature to 400 °C ($2Pt/ZrO_2$-800-R400), which was used to further reduce the Pt species, led to even worse activity (12% glycerol conversion, Entry 4, Table 3). It should be noted that for the two catalysts prepared by calcination at 800 °C, the efficiency of transfer hydrogenation was just around 1%, which means that almost none of the hydrogen from glycerol was transferred to cyclohexene. The low activity of these two catalysts can be correlated to the observed large Pt nanoparticles present in the material already prior to reduction (see Figure 4), which implies that a low fraction of the Pt atoms are exposed on the surface and thus available for catalyzing the reaction. Based on these results, it can be concluded that a calcination temperature of 550 °C leads to an optimum interaction between oxidized Pt species and ZrO_2, which then allows their reduction leading to the formation of very small Pt nanoparticles that are highly dispersed on the surface of the support and that thus display high catalytic activity.

Optimization of Pt Loading, NaOH Amount, and Reaction Temperature. Catalysts with different loadings of Pt on ZrO_2 were also tested to investigate the effects of this parameter on the catalytic performance. The same nominal molar ratio Pt/glycerol (1/1950) was used in all reactions; that is, different weights of Pt/ZrO_2 catalyst were employed. The conversion of glycerol and the yield of lactic acid improved upon an increase in the loading of Pt from 0.5 to 2%, whereas further increase of the loading to 5 and 9% caused a drop of activity (Figure 6). In all these tests, the selectivity toward lactic acid was higher than 97%, with very minor yields (≤0.2%) of side products, that is, glyceric acid, glycolic acid, and propanediol. The yield of cyclohexane from the transfer hydrogenation reaction was in the same range with all catalyst (between 16 and 20%). The results can be rationalized considering that at lower loading of Pt (0.5 and 1%), the larger

DOI: 10.1021/acscatal.9b02139
ACS Catal. 2019, 9, 9953−9963

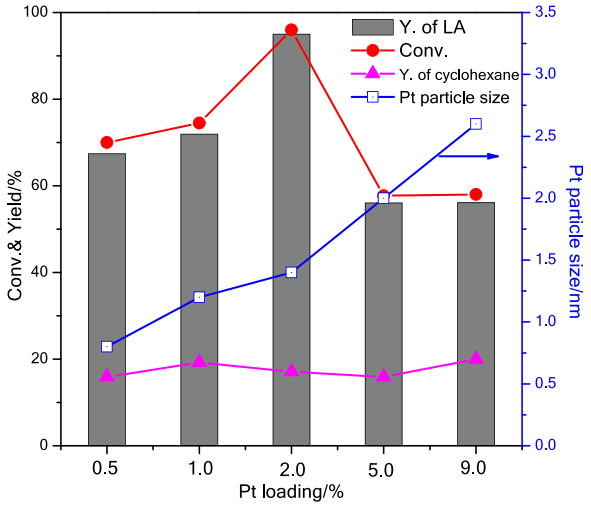

Figure 6. Catalytic performance of Pt/ZrO_2-550-R250 catalysts with different Pt loadings (0.5−9%). Reaction conditions: aqueous glycerol solution: 10 mmol (0.5 M, 20 mL); cyclohexene: 20 mmol; nominal Pt/glycerol ratio = 1/1950; NaOH: 15 mmol; temperature: 160 °C; reaction time: 4.5 h; N_2 pressure: 20 bar.

total mass of support employed might hinder the accessibility of the Pt nanoparticles,[11] whereas at higher loading of Pt (5 and 9%) the larger size and worse dispersion of the Pt nanoparticles on the ZrO_2 surface (Figure S6) account for the lower activity of the catalysts. The intermediate loading of Pt (2%) provided the best balance between these two factors, leading to the observed highest activity with $2Pt/ZrO_2$-550-R250. An alternative or additional explanation for the better performance of the 2% catalyst compared to those with lower loading is that the 2% Pt catalyst (with Pt particle size of 1.4 nm) displays the largest fraction of suitable metallic sites for the dehydrogenation of glycerol.

All the catalytic tests were conducted in the presence of NaOH. The role of this strong base was studied by varying the molar ratio between NaOH and glycerol (from 0 to 2) in the reaction mixture (Figure S8). Without addition of NaOH, both the conversion of glycerol and the selectivity to lactic acid were very low (conversion of glycerol: 1.3%). When increasing the molar ratio between NaOH and glycerol, the conversion of glycerol gradually increased, reaching 96% with 99% selectivity toward lactic acid at NaOH/glycerol = 1.5. However, a further increase in the NaOH/glycerol molar ratio to 2 caused a decrease in the conversion of glycerol to 73%, suggesting that excess NaOH can inhibit the activity of the catalyst. These results confirm that the presence of a NaOH in the reaction mixture is critical to promote the deprotonation of one of the hydroxyl groups of glycerol, thus promoting the dehydrogenation of glycerol on the surface of the Pt nanoparticles.[9,17,58,59] Moreover, NaOH can catalyze the isomerization of glyceraldehyde and dihydroxyacetone and reacts with the formed lactic acid to yield sodium lactate (which is very stable in the reaction system) thus shifting the equilibrium concentrations toward the products (Scheme 1) and granting very high selectivity toward the lactic acid salt.[9,17,18,21] A reference reaction with only NaOH and no Pt catalyst gave very low conversion of glycerol (7.3%), which is significantly lower compared to the conversion achieved in the presence of the $2Pt/ZrO_2$-550-R250 catalyst (96%). This demonstrates the crucial role played by the Pt/ZrO_2 catalyst under the relatively mild reaction conditions employed here.[17−21]

The $2Pt/ZrO_2$-550-R250 catalyst was further tested at different temperatures (from 120 to 180 °C). By increasing the reaction temperature, the expected trend of increasing glycerol conversion was observed, going from 25% at 120 °C to full conversion at 180 °C. The selectivity to lactic acid was nearly constant and always >95% with very similar side products distribution in all cases (Table S2). Also the conversion of cyclohexene and the yield of cyclohexane increased with the temperature. On the other hand, the selectivity of transfer hydrogenation did not show a clear trend as a function of the reaction temperature, reaching the highest efficiency in the reaction carried out at 140 °C.

Detailed Study of Trans-Hydrogenation Process. The catalytic results presented in Tables 2 and 3 show that only a fraction of the hydrogen atoms removed from glycerol are employed in the transfer hydrogenation of cyclohexene. This is probably due to the intrinsic low reactivity of the double bond in cyclohexene but also to the hydrophilicity of the Pt/ZrO_2 catalysts, which causes them to be preferentially located in the aqueous phase of the reaction mixture (consisting of water and glycerol), thus limiting the contact with cyclohexene (which together with cyclohexane constitutes the organic phase). As a consequence, the rate of the hydrogenation step is lower than that of the dehydrogenation. Though combining the conversion of glycerol to the transfer hydrogenation of cyclohexene is attractive, it is also interesting to evaluate the catalytic performance of the best catalyst identified in this work ($2Pt/ZrO_2$-550-R250) in the absence of cyclohexene. The test was carried out under conditions (reaction at 140 °C) at which the conversion of glycerol would be far from being complete. The results demonstrate that the presence of cyclohexene as hydrogen acceptor does not affect the catalytic performance, as both reactions showed nearly the same conversion of glycerol and yield of lactic acid (Table S3). To further investigate the formation of free H_2 in our system, we conducted an additional experiment with no hydrogen acceptor, higher amount of glycerol, and lower N_2 pressure (3 bar) (Table S4). Under these conditions, the reaction generated 10 bar free H_2 after reaction, which corresponds to 98% yield relative to the glycerol conversion. This experiment demonstrated that the dehydrogenation of glycerol did lead to the formation of free H_2.

Additionally, a linear alkene and a linear alkyne were also studied as hydrogen acceptors, instead of cyclohexene (Table S5). When 1-decene was used as hydrogen acceptor, the $2Pt/ZrO_2$-550-R250 catalyst exhibited very high activity (glycerol conversion 97%) and selectivity toward the lactic acid salt (99%). Moreover, the selectivity of the transfer-hydrogenation (92%) was much higher than with cyclohexene as hydrogen acceptor. This is probably due to the better accessibility of the C−C double bond in the linear 1-decene. On the other hand, when 1-decyne was used as the hydrogen acceptor, the catalytic activity of $2Pt/ZrO_2$-550-R250 was almost fully inhibited (1.3% glycerol conversion). This indicates that 1-decyne cannot be used as hydrogen acceptor in this system (i.e., under basic hydrothermal conditions), possibly due to poisoning of the Pt catalyst.

Kinetic Test. The reaction was monitored as a function of reaction time with catalyst $2Pt/ZrO_2$-550-R250. This test showed that under the employed conditions the reaction behaves as being first order with respect to glycerol (Figure 7).

DOI: 10.1021/acscatal.9b02139
ACS Catal. 2019, 9, 9953−9963

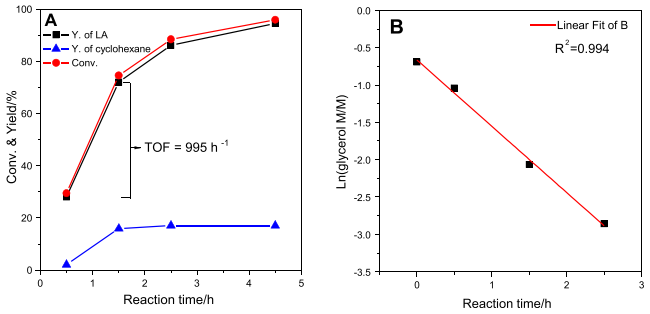

Figure 7. Conversion of glycerol and transfer hydrogenation over the 2Pt/ZrO_2-550-R250 catalyst as a function of reaction time (A); and linear fitting of the natural logarithm of the concentration of glycerol as a function of the reaction time (B). Reaction conditions: aqueous glycerol solution: 10 mmol (0.5 M, 20 mL); cyclohexene: 20 mmol; nominal Pt/glycerol ratio = 1/1950; NaOH: 15 mmol; temperature: 160 °C; N_2 pressure: 20 bar.

The turnover frequency for the conversion of glycerol based on the amount of Pt and calculated from the linear part of the kinetic curve (i.e., the first 1.5 h) was 995 h^{-1}. The selectivity toward lactic acid was >95% at all stages, which can be related to the rapid conversion of the dihydroxyacetone and/or glyceraldehyde formed from the dehydrogenation of glycerol into the lactic acid salt (see Scheme 1). The yield of cyclohexane via the transfer hydrogenation reaction increased within the first 1.5 h, after which it remained nearly constant.

Reusability. The best catalyst identified in this work, 2Pt/ZrO_2-550-R250, was selected for a reusability test (Figure 8A).

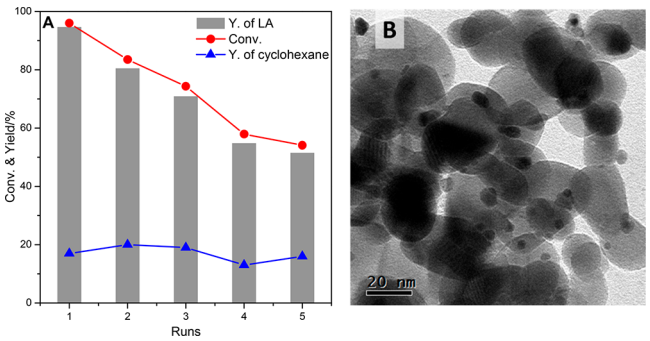

Figure 8. Reusability test of the 2Pt/ZrO_2-550-R250 catalyst for the conversion of glycerol and transfer hydrogenation: (A) Catalytic performance upon recycling; the solid catalyst was recovered by filtration, washed with water and ethanol, and dried at 100 °C after each run. (B) TEM picture of the catalyst after 5 recycles; average particle size of Pt: 4.6 nm. Reaction conditions: aqueous glycerol solution: 10 mmol (0.5 M, 20 mL); cyclohexene: 20 mmol; nominal Pt/glycerol ratio = 1/1950; NaOH: 15 mmol; temperature: 160 °C; reaction time: 4.5 h; N_2 pressure: 20 bar.

The catalyst was reused in five consecutive runs, displaying a partial and gradual loss of activity, corresponding to a decrease in glycerol conversion from 96% in the first run to 54% in the fifth run. The selectivity toward the lactic acid salt remained very high (>97%) in all runs. In addition, the yield of cyclohexane from the transfer hydrogenation was about constant for the five runs. The observed decrease in activity in the conversion of glycerol is attributed to an increase in the size of the Pt nanoparticles from 1.4 nm in the fresh catalyst to 4.6 nm after the fifth run, as evidenced by TEM analysis (Figure 8B). Such aggregation of Pt nanoparticles led to lower exposed Pt surface and thus to the observed decrease in activity.

CONCLUSIONS

We developed a novel catalytic system based on highly dispersed Pt species supported on nanosized ZrO_2 with high activity and selectivity for the one-pot conversion of glycerol into lactic acid (salt), with concomitant transfer hydrogenation of cyclohexene to cyclohexane. Careful tuning of the synthesis method through optimization of the calcination temperature, the reduction temperature, and the loading of Pt allowed the preparation of subnanometer Pt clusters and atomically dispersed Pt species (as Pt^{2+} and Pt^{4+}), which were converted into extra-fine Pt nanoparticles upon reduction. The most active catalyst (prepared by calcination at 550 °C and reduction at 250 °C) was not the material with the smallest size of the Pt domains but the one that combined a high dispersion of nanoparticles with a narrow size distribution centered at 1.4 nm with a relatively large loading of Pt (2 wt %) on the nanosized ZrO_2 support. This 2Pt/ZrO_2-550-R250 catalyst exhibited very high activity (96% glycerol conversion) and selectivity toward lactic acid salt (99%) at 160 °C and 4.5 h under N_2 atmosphere and in the presence of NaOH. This reaction also gave a 36% selectivity in the transfer-hydrogenation from glycerol to cyclohexene. The transfer hydrogenation concept could also be employed with 1-decene, achieving similarly high glycerol conversion (97%) and selectivity toward sodium lactate (99%) but significantly higher selectivity in the transfer-hydrogenation (92%). Aggregation of the very fine Pt nanoparticles into larger ones (ca. 5 nm) caused a partial deactivation of the catalyst upon reuse.

In perspective, the straightforward method introduced here allows producing catalysts with highly dispersed Pt nanoparticles with tunable size between 0.8 nm (at 0.5 wt % Pt) and 2.6 nm (at 9 wt % Pt) that are expected to display enhanced activity in several hydrogenation or dehydrogenation reactions.[33,60]

ASSOCIATED CONTENT

Supporting Information

The Supporting Information is available free of charge on the ACS Publications website at DOI: 10.1021/acscatal.9b02139.

Figure S1. Supplementary STEM images for 2Pt/ZrO_2-550. Figure S2. TEM images of 2Pt/ZrO_2 catalysts calcined and reduced with different procedures. Figure S3. STEM images of 0.5Pt/ZrO_2 catalysts calcined at different temperatures. Figure S4. STEM images coupling with EDX-mapping of 0.5Pt/ZrO_2-800. Figure S5. TEM images of Pt/ZrO_2 catalysts with different loading after calcination at 550 °C. Figure S6. TEM images of Pt/ZrO_2 catalysts with different loading after calcination at 550 °C and reduction at 250 °C. Figure S7. XRD patterns of calcined ZrO_2 and Pt/ZrO_2 catalysts with various Pt loadings. Figure S8. Effect of the amount of NaOH on the catalytic performance of 2Pt/ZrO_2-550-R250. Table S1. Catalytic conversion of glycerol to lactic acid using Pt catalysts supported on different oxides. Table S2. Catalytic conversion of glycerol to lactic acid using a Pt/ZrO_2 catalyst at different reaction temperatures. Table S3. Catalytic conversion of glycerol to lactic acid using a Pt/ZrO_2

DOI: 10.1021/acscatal.9b02139
ACS Catal. 2019, 9, 9953−9963

catalyst, as a function of the presence of cyclohexene. Table S4. Catalytic conversion of glycerol to lactic acid using 2Pt/ZrO_2-550-R250. Table S5. Catalytic conversion of glycerol over 2Pt/ZrO_2-550-R250 in the presence of 1-decene or 1-decyne as hydrogen acceptor (PDF)

AUTHOR INFORMATION

Corresponding Author

E-mail: p.p.pescarmona@rug.nl.

ORCID

Sara Bals: 0000-0002-4249-8017

Paolo P. Pescarmona: 0000-0003-3608-6400

Author Contributions

The manuscript was written through contributions of all authors. All authors have given approval to the final version of the manuscript.

Notes

The authors declare no competing financial interest.

ACKNOWLEDGMENTS

Zhenchen Tang acknowledges the financial support from the China Scholarship Council for his Ph.D. grant. All the authors are grateful for the technical support from Erwin Wilbers, Anne Appeldoorn, and Marcel de Vries, the TEM support from Dr. Marc Stuart, and the ICP-OES support from Johannes van der Velde. Pei Liu and Sara Bals acknowledge financial support from the European Commission under the Horizon 2020 Programme by means of grant agreement No. 731019 EUSMI.

REFERENCES

(1) Corma, A.; Iborra, S.; Velty, A. Chemical routes for the transformation of biomass into chemicals. *Chem. Rev.* **2007**, *107* (6), 2411−2502.

(2) Huber, G. W.; Iborra, S.; Corma, A. Synthesis of Transportation Fuels from Biomass: Chemistry, Catalysts, and Engineering. *Chem. Rev.* **2006**, *106* (9), 4044−4098.

(3) Besson, M.; Gallezot, P.; Pinel, C. Conversion of biomass into chemicals over metal catalysts. *Chem. Rev.* **2014**, *114* (3), 1827−70.

(4) Zhou, C. H.; Beltramini, J. N.; Fan, Y. X.; Lu, G. Q. Chemoselective catalytic conversion of glycerol as a biorenewable source to valuable commodity chemicals. *Chem. Soc. Rev.* **2008**, *37* (3), 527−49.

(5) Alonso, D. M.; Wettstein, S. G.; Dumesic, J. A. Bimetallic catalysts for upgrading of biomass to fuels and chemicals. *Chem. Soc. Rev.* **2012**, *41* (24), 8075−98.

(6) Behr, A.; Eilting, J.; Irawadi, K.; Leschinski, J.; Lindner, F. Improved utilisation of renewable resources: New important derivatives of glycerol. *Green Chem.* **2008**, *10* (1), 13−30.

(7) Ito, T.; Nakashimada, Y.; Senba, K.; Matsui, T.; Nishio, N. Hydrogen and ethanol production from glycerol-containing wastes discharged after biodiesel manufacturing process. *J. Biosci. Bioeng.* **2005**, *100* (3), 260−265.

(8) Huber, G. W.; Shabaker, J. W.; Dumesic, J. A. Raney Ni-Sn Catalyst for H_2 Production from Biomass-Derived Hydrocarbons. *Science* **2003**, *300* (5628), 2075−2077.

(9) Dusselier, M.; Van Wouwe, P.; Dewaele, A.; Makshina, E.; Sels, B. F. Lactic acid as a platform chemical in the biobased economy: the role of chemocatalysis. *Energy Environ. Sci.* **2013**, *6* (5), 1415−1442.

(10) Cho, H. J.; Chang, C.-C.; Fan, W. Base free, one-pot synthesis of lactic acid from glycerol using a bifunctional Pt/Sn-MFI catalyst. *Green Chem.* **2014**, *16* (7), 3428−3433.

(11) Tang, Z.; Fiorilli, S. L.; Heeres, H. J.; Pescarmona, P. P. Multifunctional Heterogeneous Catalysts for the Selective Conversion of Glycerol into Methyl Lactate. *ACS Sustainable Chem. Eng.* **2018**, *6* (8), 10923−10933.

(12) Tang, Z.; Deng, W.; Wang, Y.; Zhu, E.; Wan, X.; Zhang, Q.; Wang, Y. Transformation of cellulose and its derived carbohydrates into formic and lactic acids catalyzed by vanadyl cations. *ChemSusChem* **2014**, *7* (6), 1557−1567.

(13) Lin, Y.-C. Catalytic valorization of glycerol to hydrogen and syngas. *Int. J. Hydrogen Energy* **2013**, *38* (6), 2678−2700.

(14) Wawrzetz, A.; Peng, B.; Hrabar, A.; Jentys, A.; Lemonidou, A. A.; Lercher, J. A. Towards understanding the bifunctional hydrodeoxygenation and aqueous phase reforming of glycerol. *J. Catal.* **2010**, *269* (2), 411−420.

(15) Lubitz, W.; Tumas, W. Hydrogen: An Overview. *Chem. Rev.* **2007**, *107* (10), 3900−3903.

(16) Cortright, R. D.; Davda, R. R.; Dumesic, J. A. Hydrogen from catalytic reforming of biomass-derived hydrocarbons in liquid water. *Nature* **2002**, *418*, 964−967.

(17) Shen, Y.; Zhang, S.; Li, H.; Ren, Y.; Liu, H. Efficient synthesis of lactic acid by aerobic oxidation of glycerol on Au-Pt/TiO_2 catalysts. *Chem. - Eur. J.* **2010**, *16* (25), 7368−7371.

(18) Purushothaman, R. K. P.; van Haveren, J.; van Es, D. S.; Melián-Cabrera, I.; Meeldijk, J. D.; Heeres, H. J. An efficient one pot conversion of glycerol to lactic acid using bimetallic gold-platinum catalysts on a nanocrystalline CeO_2 support. *Appl. Catal., B* **2014**, *147*, 92−100.

(19) Kishida, H.; Jin, F.; Zhou, Z.; Moriya, T.; Enomoto, H. Conversion of Glycerin into Lactic Acid by Alkaline Hydrothermal Reaction. *Chem. Lett.* **2005**, *34* (11), 1560−1561.

(20) Maris, E.; Davis, R. Hydrogenolysis of glycerol over carbon-supported Ru and Pt catalysts. *J. Catal.* **2007**, *249* (2), 328−337.

(21) Auneau, F.; Arani, L. S.; Besson, M.; Djakovitch, L.; Michel, C.; Delbecq, F.; Sautet, P.; Pinel, C. Heterogeneous Transformation of Glycerol to Lactic Acid. *Top. Catal.* **2012**, *55* (7−10), 474−479.

(22) Tavor, D.; Gefen, I.; Dlugy, C.; Wolfson, A. Transfer Hydrogenations of Nitrobenzene Using Glycerol as Solvent and Hydrogen Donor. *Synth. Commun.* **2011**, *41* (22), 3409−3416.

(23) Wolfson, A.; Dlugy, C.; Shotland, Y.; Tavor, D. Glycerol as solvent and hydrogen donor in transfer hydrogenation−dehydrogenation reactions. *Tetrahedron Lett.* **2009**, *50* (43), 5951−5953.

(24) Gilkey, M. J.; Xu, B. Heterogeneous Catalytic Transfer Hydrogenation as an Effective Pathway in Biomass Upgrading. *ACS Catal.* **2016**, *6* (3), 1420−1436.

(25) Wang, D.; Astruc, D. The Golden Age of Transfer Hydrogenation. *Chem. Rev.* **2015**, *115* (13), 6621−6686.

(26) Yu, W.; Porosoff, M. D.; Chen, J. G. Review of Pt-Based Bimetallic Catalysis: From Model Surfaces to Supported Catalysts. *Chem. Rev.* **2012**, *112* (11), 5780−5817.

(27) Bamwenda, G. R.; Tsubota, S.; Nakamura, T.; Haruta, M. The influence of the preparation methods on the catalytic activity of platinum and gold supported on TiO_2 for CO oxidation. *Catal. Lett.* **1997**, *44* (1), 83−87.

(28) Barias, O. A.; Holmen, A.; Blekkan, E. A. Propane Dehydrogenation over Supported Pt and Pt−Sn Catalysts: Catalyst Preparation, Characterization, and Activity Measurements. *J. Catal.* **1996**, *158* (1), 1−12.

(29) Li, Y.; Tang, L.; Li, J. Preparation and electrochemical performance for methanol oxidation of Pt/graphene nanocomposites. *Electrochem. Commun.* **2009**, *11* (4), 846−849.

(30) Lordi, V.; Yao, N.; Wei, J. Method for Supporting Platinum on Single-Walled Carbon Nanotubes for a Selective Hydrogenation Catalyst. *Chem. Mater.* **2001**, *13* (3), 733−737.

(31) Wei, S.; Li, A.; Liu, J.-C.; Li, Z.; Chen, W.; Gong, Y.; Zhang, Q.; Cheong, W.-C.; Wang, Y.; Zheng, L.; Xiao, H.; Chen, C.; Wang, D.; Peng, Q.; Gu, L.; Han, X.; Li, J.; Li, Y. Direct observation of noble metal nanoparticles transforming to thermally stable single atoms. *Nat. Nanotechnol.* **2018**, *13* (9), 856−861.

(32) Jones, J.; Xiong, H.; DeLaRiva, A. T.; Peterson, E. J.; Pham, H.; Challa, S. R.; Qi, G.; Oh, S.; Wiebenga, M. H.; Pereira Hernández, X.

DOI: 10.1021/acscatal.9b02139
ACS Catal. 2019, 9, 9953−9963

I.; Wang, Y.; Datye, A. K. Thermally stable single-atom platinum-on-ceria catalysts via atom trapping. *Science* **2016**, *353* (6295), 150−154.
(33) Xiong, H.; Lin, S.; Goetze, J.; Pletcher, P.; Guo, H.; Kovarik, L.; Artyushkova, K.; Weckhuysen, B. M.; Datye, A. K. Thermally Stable and Regenerable Platinum−Tin Clusters for Propane Dehydrogenation Prepared by Atom Trapping on Ceria. *Angew. Chem., Int. Ed.* **2017**, *56* (31), 8986−8991.
(34) Xie, P.; Pu, T.; Nie, A.; Hwang, S.; Purdy, S. C.; Yu, W.; Su, D.; Miller, J. T.; Wang, C. Nanoceria-Supported Single-Atom Platinum Catalysts for Direct Methane Conversion. *ACS Catal.* **2018**, *8* (5), 4044−4048.
(35) Nie, L.; Mei, D.; Xiong, H.; Peng, B.; Ren, Z.; Hernandez, X. I. P.; DeLaRiva, A.; Wang, M.; Engelhard, M. H.; Kovarik, L.; Datye, A. K.; Wang, Y. Activation of surface lattice oxygen in single-atom Pt/CeO_2 for low-temperature CO oxidation. *Science* **2017**, *358* (6369), 1419−1423.
(36) Thang, H. V.; Pacchioni, G.; DeRita, L.; Christopher, P. Nature of stable single atom Pt catalysts dispersed on anatase TiO_2. *J. Catal.* **2018**, *367*, 104−114.
(37) Mullins, D. R. The surface chemistry of cerium oxide. *Surf. Sci. Rep.* **2015**, *70* (1), 42−85.
(38) Wang, A.; Li, J.; Zhang, T. Heterogeneous single-atom catalysis. *Nat. Rev. Chem.* **2018**, *2* (6), 65−81.
(39) Kwon, Y.; Kim, T. Y.; Kwon, G.; Yi, J.; Lee, H. Selective Activation of Methane on Single-Atom Catalyst of Rhodium Dispersed on Zirconia for Direct Conversion. *J. Am. Chem. Soc.* **2017**, *139* (48), 17694−17699.
(40) Yang, X.-F.; Wang, A.; Qiao, B.; Li, J.; Liu, J.; Zhang, T. Single-Atom Catalysts: A New Frontier in Heterogeneous Catalysis. *Acc. Chem. Res.* **2013**, *46* (8), 1740−1748.
(41) Hwang, K.-R.; Ihm, S.-K.; Park, S.-C.; Park, J.-S. Pt/ZrO_2 catalyst for a single-stage water-gas shift reaction: Ti addition effect. *Int. J. Hydrogen Energy* **2013**, *38* (14), 6044−6051.
(42) Zhu, Y.; An, Z.; He, J. Single-atom and small-cluster Pt induced by Sn (IV) sites confined in an LDH lattice for catalytic reforming. *J. Catal.* **2016**, *341*, 44−54.
(43) Moliner, M.; Gabay, J. E.; Kliewer, C. E.; Carr, R. T.; Guzman, J.; Casty, G. L.; Serna, P.; Corma, A. Reversible Transformation of Pt Nanoparticles into Single Atoms inside High-Silica Chabazite Zeolite. *J. Am. Chem. Soc.* **2016**, *138* (48), 15743−15750.
(44) Lang, R.; Xi, W.; Liu, J.-C.; Cui, Y.-T.; Li, T.; Lee, A. F.; Chen, F.; Chen, Y.; Li, L.; Li, L.; Lin, J.; Miao, S.; Liu, X.; Wang, A.-Q.; Wang, X.; Luo, J.; Qiao, B.; Li, J.; Zhang, T. Non defect-stabilized thermally stable single-atom catalyst. *Nat. Commun.* **2019**, *10* (1), 234.
(45) Ho, L.; Hwang, C.; Lee, J.; Wang, I.; Yeh, C. Reduction of platinum dispersed on dealuminated beta zeolite. *J. Mol. Catal. A: Chem.* **1998**, *136* (3), 293−299.
(46) Park, S. H.; Tzou, M. S.; Sachtler, W. M. H. Temperature programmed reduction and re-oxidation of platinum in y-zeolites. *Appl. Catal.* **1986**, *24* (1), 85−98.
(47) Foger, K.; Jaeger, H. Redispersion of Pt—zeolite catalysts with chlorine. *Appl. Catal.* **1989**, *56* (1), 137−147.
(48) Hoang, D. L.; Farrage, S. A. F.; Radnik, J.; Pohl, M. M.; Schneider, M.; Lieske, H.; Martin, A. A comparative study of zirconia and alumina supported Pt and Pt−Sn catalysts used for dehydrocyclization of n-octane. *Appl. Catal., A* **2007**, *333* (1), 67−77.
(49) Zhu, L.; Lu, J.; Chen, P.; Hong, X.; Xie, G.; Hu, G.; Luo, M. A comparative study on Pt/CeO_2 and Pt/ZrO_2 catalysts for crotonaldehyde hydrogenation. *J. Mol. Catal. A: Chem.* **2012**, *361*−*362*, 52−57.
(50) Dall'Agnol, C.; Gervasini, A.; Morazzoni, F.; Pinna, F.; Strukul, G.; Zanderighi, L. Hydrogenation of carbon monoxide: Evidence of a strong metal-support interaction in $RhZrO_2$ catalysts. *J. Catal.* **1985**, *96* (1), 106−114.
(51) Hoang, D. L.; Berndt, H.; Lieske, H. Hydrogen spillover phenomena on Pt/ZrO_2. *Catal. Lett.* **1995**, *31* (2), 165−172.
(52) Querino, P. S.; Bispo, J. R. C.; Rangel, M. d. C. The effect of cerium on the properties of Pt/ZrO_2 catalysts in the WGSR. *Catal. Today* **2005**, *107*−*108*, 920−925.
(53) Giordano, F.; Trovarelli, A.; de Leitenburg, C.; Giona, M. A Model for the Temperature-Programmed Reduction of Low and High Surface Area Ceria. *J. Catal.* **2000**, *193* (2), 273−282.
(54) Hatanaka, M.; Takahashi, N.; Tanabe, T.; Nagai, Y.; Dohmae, K.; Aoki, Y.; Yoshida, T.; Shinjoh, H. Ideal Pt loading for a Pt/CeO_2-based catalyst stabilized by a Pt−O−Ce bond. *Appl. Catal., B* **2010**, *99* (1), 336−342.
(55) Castillo Martinez, F. A.; Balciunas, E. M.; Salgado, J. M.; Domínguez González, J. M.; Converti, A.; Oliveira, R. P. d. S. Lactic acid properties, applications and production: A review. *Trends Food Sci. Technol.* **2013**, *30* (1), 70−83.
(56) Wang, J.; Li, Q.; Yao, J. The effect of metal−acid balance in Pt-loading dealuminated Y zeolite catalysts on the hydrogenation of benzene. *Appl. Catal., A* **1999**, *184* (2), 181−188.
(57) Akiyama, M.; Sato, S.; Takahashi, R.; Inui, K.; Yokota, M. Dehydration−hydrogenation of glycerol into 1,2-propanediol at ambient hydrogen pressure. *Appl. Catal., A* **2009**, *371* (1−2), 60−66.
(58) Zhang, Y.; Shen, Z.; Zhou, X.; Zhang, M.; Jin, F. Solvent isotope effect and mechanism for the production of hydrogen and lactic acid from glycerol under hydrothermal alkaline conditions. *Green Chem.* **2012**, *14* (12), 3285−3288.
(59) Razali, N.; Abdullah, A. Z. Production of lactic acid from glycerol via chemical conversion using solid catalyst: A review. *Appl. Catal., A* **2017**, *543*, 234−246.
(60) Wei, H.; Liu, X.; Wang, A.; Zhang, L.; Qiao, B.; Yang, X.; Huang, Y.; Miao, S.; Liu, J.; Zhang, T. FeOx-supported platinum single-atom and pseudo-single-atom catalysts for chemoselective hydrogenation of functionalized nitroarenes. *Nat. Commun.* **2014**, *5*, 5634−5641.

DOI: 10.1021/acscatal.9b02139
ACS Catal. 2019, 9, 9953−9963